Fundamental Studies on Earthquake Response of a Long Span Suspension Bridge

KONISHI, Ichiro; YAMADA, Yoshikazu

Fundamental Studies on Earthquake Response of a Long Span Suspension Bridge

By

Ichiro KONISHI* and Yoshikazu YAMADA*

(Received April 30, 1960)

This paper deals theoretically with the earthquake response of a long span suspension bridge. An exact solution of this problem is seldom possible because of the complexity of the structure and the earthquake motions. For the convenience of the analysis a simplified structural system of the suspension bridge with finite degrees of freedom of motion is adopted, and the ground disturbances are assumed to be a simple shape. To simplify the problem, linearized deflection theory of suspension bridges is employed. Some parts of numerical calculation, natural frequencies and modes of the system, had been done on a high speed digital computer. On this investigation some response spectra are given, and the fundamental earthquake response characteristics of the suspension bridge are made clear.

1. Introduction

Problems on aerodynamic stability of suspension bridges have been investigated by many specialists during the past few decades, but there are few investigation and technical papers on earthquake response of suspension bridges. In this paper, a method of analysing the earthquake response of a long span suspension bridge is presented, and the fundamental dynamic characteristics of the suspension bridge to earthquake are investigated.

Because of the complexity of the structure, it is seldom possible to obtain an exact solution of the problem. In this investigation, the suspension bridge will be simplified into a physically analogous system to which the theory of finite degrees of freedom can be applied. The earthquake motions being also quite complicated are assumed to be of a simple shape. Only the effects of ground motions acting in the direction of the bridge axis will be treated in this paper. In the analysis of earthquake response of the suspension bridge, the effects of the stiffness and masses of the towers are of significant importance, and both effects are taken into account in this analysis.

* Department of Civil Engineering

Numerical calculations will be done on the Akashi Straits Bridge which is now being planned by Kobe City Authority.

2. Physical System Considered

The system considered is as shown in Fig. 1. Stiffening frames of the suspension bridge consist of rigid bars connected with elastic hinges. Elastic constants

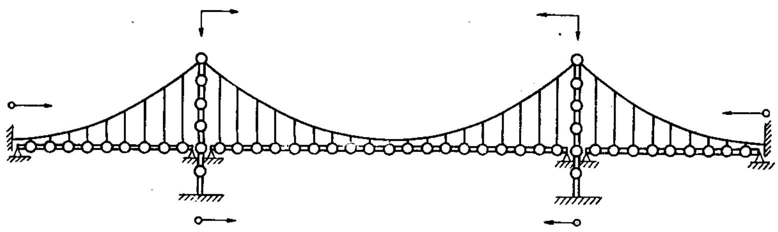

Fig. 1. Physical System Considered.

of the hinges are so selected that the analogy of bending characteristics to the original stiffening frame might be satisfied. Dead weight of the stiffening frames, floor systems, and cables are assumed to be concentrated at the hinged points considered. Each hinged point has a single degree of freedom of motion to the vertical direction specified by a deflection coordinate y_r.

Towers of the bridge are also replaced by the same physically analogous system. Only the horizontal motion is assumed to be allowable to the points in the towers. Axial forces and horizontal forces acting to the top of the towers are taken into consideration.

Ordinary assumptions in the analysis of suspension bridges, such as suspenders being inextensible, are assumed in this analysis. Vibration damping of the structure is omitted in the analysis.

Using such simplified system, theory of system having finite degrees of freedom can be applied to the problem[1]. When the suspension bridge is devided into fairly large number of segments, a good approximation is obtained. Only high speed computers can execute numerical calculations for the analysis of such system.

3. Equations of Motion

(a) Stiffening Frames

A point considered here is the elastic hinged point of the system specified above, and the dead load is assumed to be concentrated in this point. In Fig. 2, three adjoining points in the stiffening frame are shown, and the equilibrium of the point r will be discussed here. Solid lines in Fig. 2 show the condition of

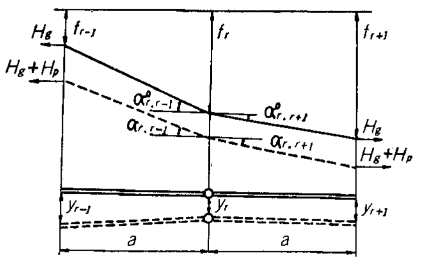

Fig. 2.

static equilibrium due to dead load. As the stiffening frames of suspension bridges carry no dead weight, the following static equilibrium is derived regarding the point r.

$$\tan \alpha^0_{r,r+1} - \tan \alpha^0_{r,r-1} = (W_r/H_g) \qquad (1)$$

where, H_g: horizontal component of dead load cable tension, W_r: dead load concentrated at the point r. Using cable sag of three points, Eq. (1) is

$$(f_{r-1} - 2f_r + f_{r+1})/a = -(W_r/H_g)\,. \qquad (2)$$

Two kinds of internal reactions take place with the displacement of the point. One is due to bending of stiffening frame, and the other is due to increment of the cable tension.

Reaction due to the bending of stiffening frame is

$$R^M_r = (M_{r-1} - 2M_r + M_{r+1})/a\,. \qquad (3)$$

where, M_r: bending moment at the point r in the stiffening frame, R^M_r: reaction due to bending moment of the stiffening frame. Moment M_r is assumed to be expressed by the deflections of three adjoining points in the stiffening frame as

$$M_r = -(B_r/a)(y_{r-1} - 2y_r + y_{r+1}) \qquad (4)$$

where, B_r: elastic constant, selected to satisfy the physical conditions.

With the increment in cable stress due to vibration, horizontal component of cable stress increases from H_g to $H_g + H_p$. Reaction due to cable tension $H_g + H_p$ is,

$$R^{H_g+H_p}_r = (H_g + H_p)(\tan \alpha_{r,r+1} - \tan \alpha_{r,r-1}) \qquad (5)$$

in which,

$$\left.\begin{aligned} \tan \alpha_{r,r-1} &= \{(f_r + y_r) - (f_{r-1} + y_{r-1})\}/a \\ \tan \alpha_{r,r+1} &= \{(f_{r+1} + y_{r+1}) - (f_r + y_r)\}/a\,. \end{aligned}\right\} \qquad (6)$$

Substituting Eq. (6) into Eq(5), and using the relation of Eq. (2), the reaction due to increment of cable tension is

$$\begin{aligned} R^{H_p}_r = {} & (H_p/a)(f_{r-1} - 2f_r + f_{r+1}) \\ & + \{(H_g + H_p)/a\}(y_{r-1} - 2y_r + y_{r+1})\,. \end{aligned} \qquad (7)$$

Total reaction at the point r due to the deflections of the stiffening frame is, therefore,

$$\begin{aligned} R_r = {} & (1/a)(M_{r-1} - 2M_r + M_{r+1}) \\ & + (H_p/a)(f_{r-1} - 2f_r + f_{r+1}) \\ & + \{(H_g + H_p)/a\}(y_{r-1} - 2y_r + y_{r+1})\,. \end{aligned} \qquad (8)$$

No external forces being applied to the point r, the equation of motion of the point r is given as

$$(W_r/g)\ddot{y}_r = (1/a)(M_{r-1}-2M_r+M_{r+1}) + (H_p/a)(f_{r-1}-2f_r+f_{r+1}) + \{(H_g+H_p)/a\}(y_{r-1}-2y_r+y_{r+1}) \ . \tag{9}$$

(b) Cable Equation

The increment of horizontal component of cable tension, H_p, in Eq. (9) is the function of deflections of the stiffening frame and it can be obtained from so-called cable equation.

Assuming that the cable element $\{r, r+1\}$ moves to the position $\{r', (r+1)'\}$ as shown in Fig. 3, due to the increment of the cable tension, the following relation is given neglecting small quantities of higher order.

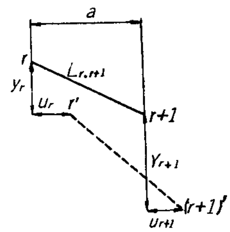

Fig. 3.

$$(u_{r+1}-u_r)\cos\alpha^0_{r,r+1}+(y_{r+1}-y_r)\sin\alpha^0_{r,r+1} = (t_{r,r+1}L_{r,r+1}/E_cA_c) \tag{10}$$

where, $t_{r,r+1}$: the increment of cable stress of the cable element $r, r+1$, $L_{r,r+1}$: length of the cable element $r, r+1$, E_c: Young's modulus of the material of the cable, A_c: cross section area of the cable, u_r: horizontal component of the displacement of the point r, y_r: vertical component of the displacement of the point r. The horizontal component of the elongation of the cable element $r, r+1$, is

$$\Delta u_{r,r+1} = u_{r+1}-u_r = (t_{r,r+1},\ L_{r,r+1}/E_cA_c\cos\alpha^0_{r,r+1}) - (y_{r+1}-y_r)\tan\alpha^0_{r,r+1} \ . \tag{11}$$

Employing H_p, and a,

$$\Delta u_{r,r+1} = (H_pa/E_cA_c\cos^3\alpha^0_{r,r+1}) - (y_{r+1}-y_r)\tan\alpha^0_{r,r+1} \ . \tag{12}$$

Total elongation of the cable is

$$u = \sum\Delta u = (H_p/E_cA_c)\sum(a/\cos^3\alpha^0_{r,r+1}) + \sum y_r(\tan\alpha^0_{r,r+1}-\tan\alpha^0_{r,r-1}) \ . \tag{13}$$

Using Eq. (2), Eq. (13) will be

$$u = (H_pL_E/E_cA_c)-(W_r/H_g)\sum y_r \tag{14}$$

where

$$L_E = \sum(a/\cos^3\alpha^0_{r,r+1}) \ . \tag{15}$$

Eq. (14) must be applied to each span of the suspension bridge, and the value of H_p is different for each span. Expressing the quantities of the left side span by suffix 1, of the center span with suffix c, and of the right side span with suffix 2, one obtains

$$\left.\begin{aligned} u_1 &= (H_{p1}L_{E1}/E_cA_c)-(W_r/H_g)\sum_{(1)} y_r \\ u_c &= (H_{pc}L_{Ec}/E_cA_c)-(W_r/H_g)\sum_{(c)} y_r \\ u_2 &= (H_{p2}L_{E2}/E_cA_c)-(W_r/H_g)\sum_{(2)} y_r\,. \end{aligned}\right\} \tag{16}$$

The following conditions must be also satisfied, taking the positive directions of horizontal displacement as in Fig. 1.

$$\left.\begin{aligned} u_1 &= y_{Tl}-Z_A \\ u_c &= -y_{Tl}-y_{Tr} \\ u_2 &= y_{Tr}-Z_D \end{aligned}\right\} \tag{17}$$

where, y_{Tl}: displacement of the top of the left side tower, y_{Tr}: displacement of the top of the right side tower, Z_A: displacement of the left side anchorage, Z_D: displacement of the right side anchorage.

(*c*) *Equation of Motion of Towers*

Towers of the suspension bridge are also divided into small segments which consist of rigid bars and elastic hinges. Fig. 4 shows the tower subjected to ground motions at the base and the horizontal and vertical forces at the top.

The same method of derivation of equation of motion as before is employed, then the equation of motion of inner points of the tower are obtained as

$$\begin{aligned}(W_r/g)\ddot{y}_r = {} & (1/b)(M_{r-1}-2M_r+M_{r+1}) \\ & -(1/b)(P_g+P_p)(y_{r-1}-2y_r+y_{r+1})\,. \end{aligned} \tag{18}$$

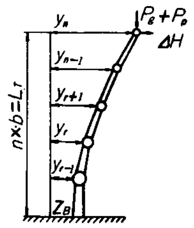

Fig. 4.

At the top of the tower the following equation is to be applied as the horizontal force ΔH is acting there.

$$(W_n/g)\ddot{y}_n = (1/b)(M_{n-1})-(1/b)(P_g+P_p)(-y_n+y_{n-1})+\Delta H \tag{19}$$

where, P_g: axial force due to dead load acting at the tower, P_p: increment to the axial force due to inertia force, ΔH: horizontal force acting at the top of the tower during vibration, due to the difference of cable tension, W_r: dead weight of the tower concentrated at the point r.

The horizontal force ΔH are given as,

$$\left.\begin{array}{ll}\Delta H_1 = H_{pc} - H_{p1} & \text{(for the left side tower)} \\ \Delta H_2 = H_{pc} - H_{p2}\,. & \text{(for the right side tower)}\end{array}\right\} \tag{20}$$

(*d*) *Linearization of the Equations*

The equation of motion derived are originally depending upon the deflection theory of suspension bridges and have non-linear characteristics. When the increment of the cable tension and of the axial force due to the inertia force are small compared to those due to dead load, terms H_g+H_p, and P_g+P_p, in Eqs. (9) and (19) are assumed to be H_g, and P_g, then the quantities having non-linear properties are ignored. Equations obtained correspond to so-called linearized deflection theory of suspension bridges[2].

(*e*) *System of the Fundamental Equation of Motion*

Using the linearized theory, and considering coupling conditions, Eqs. (17) and (20), a system of fundamental differential equations of motion of the following form can be derived.

$$[A](\ddot{y}_r)+[B](y_r)+(P_r(t)) = 0 \tag{21}$$

In Eq. (21) [ ], ( ) show a square symmetric and a vector matrix respectively, and y_r: displacement of a point in the stiffening frame, or the tower, $P_r(t)$: external force due to ground motion. Matrix $[A]$ is a diagonal matrix with the diagonal element $a_{rr}=(W_r/g)$. Matrix $[B]$ is stiffness matrix. Vector matrix of external forces $P_r(t)$ is the function of the ground motions Z_A, Z_B, Z_C, and Z_D, which are displacements of the left side anchorage, of the left side tower base, of the right side tower base, and of the right side anchorage.

The problem expressed by Eq. (21) is physically the vibration problem with multi-degrees of freedom and can be effectively solved by modal analysis of vibration if the natural frequencies and modes of vibration are obtained[4].

4. Natural Frequencies and Modes

Frequency equation of the system is

$$|[B]-\lambda\,[A]| = 0\,. \tag{22}$$

where, $\lambda=\omega^2$: characteristic values, ω: circular frequencies of the system. The characteristic roots and vectors of this determinantal equation represent the natural frequencies and modes of the system.

Matrices $[A]$ and $[B]$ in Eqs. (21) and (22) can be obtained if the simplification of the suspension bridge and the structural constants concerned are given.

As the first approximation, the system shown in Fig. 5 is adopted. Dimensions

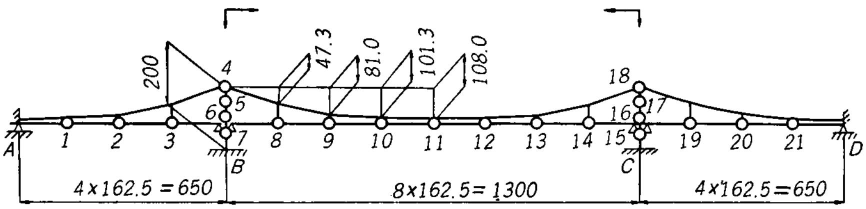

Fig. 5.

and dead loads of the system are selected refering to the values of the Akashi Straits Bridge[3]. They are,

$$a = L/8 = 1300/8 = 162.5\,\text{m}$$
$$b = L^T/4 = 200/4 = 50.0\,\text{m}$$
$$H_g = 19560\,\text{ton}$$

Weight W_r, and stiffness constant B_r are shown in Table 1. The stiffening frames are considered to have uniform cross section for each span, and towers to have varying cross sections. Numbers r of the points are given in Fig. 5.

Using these, square matrices $[A]$ and $[B]$ with 21×21 elements are obtained. Tables of these matrices are omitted here as they take much space.

Because the system of Fig. 5 is symmetric with respect to the center of the center span of the system, the natural modes of vibration are either symmetric or asymmetric, and it becomes convenient to evaluate the natural frequencies and modes in two separate groups.

Table 1. Weight and Stiffness.

Points	W_r (ton)	B_r (ton-m)
1, 21	1625	6.462×10^5
2, 20	1625	6.462×10^5
3, 19	1625	6.462×10^5
4, 18	340	0
5, 17	1165	46.158×10^5
6, 16	1778	107.52×10^5
7, 15	2521	216.05×10^5
8, 14	1625	5.169×10^5
9, 13	1625	5.169×10^5
10, 12	1625	5.169×10^5
11	1625	5.169×10^5
Tower Base		391.3×10^5

Values λ and characteristic vectors for the symmetric and asymmetric modes are given in Tables 2 and 3. Configurations of the modes are shown in Figs. 6 and 7. They were obtained on the high speed digital computer. For convenience of the following analysis, the natural modes of the system, shown in Tables 2 and 3, are normalized so as to satisfy the condition

$$\sum_{r=1}^{n} (W_r/g)(Y_r^{(i)})^2 = 1\,. \tag{23}$$

($i = 1, 2, \cdots\cdots, 11$ for symmetric modes)
($i = 1, 2, \cdots\cdots, 10$ for asymmetric modes)

Table 2. Symmetric Modes.

Modes	1	2	3	4	5	6	7	8	9	10	11
	Characteristic Values										
λ_i	.2930	1.0208	1.9928	2.0421	2.9491	4.2385	4.5435	21.734	129.83	358.37	781.86
Periods (sec)	11.608	6.2191	4.4511	4.3969	3.6588	3.0519	2.9478	1.3477	.5514	.3319	.2247
	Natural Modes, Normalized (10^{-1} m)										
$Y_1=Y_{21}$	−.1734	−.0834	−.1697	.3883	−.0203	.2901	.0122	−.0106	.0044	−.0013	−.0097
$Y_2=Y_{20}$	−.2413	−.1251	−.3042	0	−.0583	−.3626	−.0058	−.0099	.0044	−.0013	−.0097
$Y_3=Y_{19}$	−.1734	−.0834	−.1697	−.3883	−.0203	.2901	.0122	−.0106	.0044	−.0013	−.0097
$Y_4=Y_{18}$	.0547	.0156	−.0006	0	−.0059	−.0063	.0015	−.0321	.0881	−.0720	−1.193
$Y_5=Y_{17}$	.0274	.0080	−.0003	0	−.0033	−.0037	.0009	−.4501	.4377	−.1504	.0549
$Y_6=Y_{16}$	.0105	.0031	−.0001	0	−.0014	−.0016	.0004	−.3529	−.2623	.2854	−.0266
$Y_7=Y_{15}$	.0022	.0006	0	0	−.0003	−.0004	.0001	−.1110	−.2371	−.3546	.0070
$Y_8=Y_{14}$	.0934	.3100	−.1564	0	−.3845	.0208	.1543	.0107	−.0044	.0013	.0097
$Y_9=Y_{13}$	.2005	.1991	−.3092	0	.2284	.0243	−.2705	.0101	−.0044	.0013	.0097
$Y_{10}=Y_{12}$	.2864	−.2078	−.1755	0	.1195	.0027	.3620	.0102	−.0044	.0013	.0097
Y_{11}	.3192	−.4313	−.0335	0	−.4076	.0355	−.3827	.0102	−.0044	.0013	.0097

Table 3. Asymmetric Modes.

Modes	1	2	3	4	5	6	7	8	9	10
	Characteristic Values									
λ_i	.4658	.5011	1.9241	2.0421	3.8546	4.1984	21.167	125.39	350.79	430.40
Periods (sec)	9.2067	8.8771	4.5297	4.3969	3.2003	3.0666	1.3657	.5611	.3354	.3028
	Natural Modes, Normalized (10^{-1} m)									
$Y_1=-Y_{21}$	0	−.2731	0	.3883	0	.2744	−.0219	.0101	−.0072	−.0164
$Y_2=-Y_{20}$	0	−.3871	0	0	0	−.3884	−.0202	.0100	−.0072	−.0164
$Y_3=-Y_{19}$	0	−.2731	0	−.3883	0	.2744	−.0219	.0101	−.0072	−.0164
$Y_4=-Y_{18}$	0	.0763	0	0	0	−.0134	−.0640	.1960	−.3978	−1.111
$Y_5=-Y_{17}$	0	.0385	0	0	0	−.0078	−.4544	.4255	−.1064	.1421
$Y_6=-Y_{16}$	0	.0149	0	0	0	−.0034	−.3486	−.2689	.2595	−.1192
$Y_7=-Y_{15}$	0	.0031	0	0	0	−.0008	−.1087	−.2330	−.3467	.0895
$Y_8=-Y_{14}$	−.2746	0	0.3883	0	.2746	0	0	0	0	0
$Y_9=-Y_{13}$	−.3883	0	0	0	−.3883	0	0	0	0	0
$Y_{10}=-Y_{12}$	−.2746	0	−.3883	0	.2746	0	0	0	0	0
Y_{11}	0	0	0	0	0	0	0	0	0	0

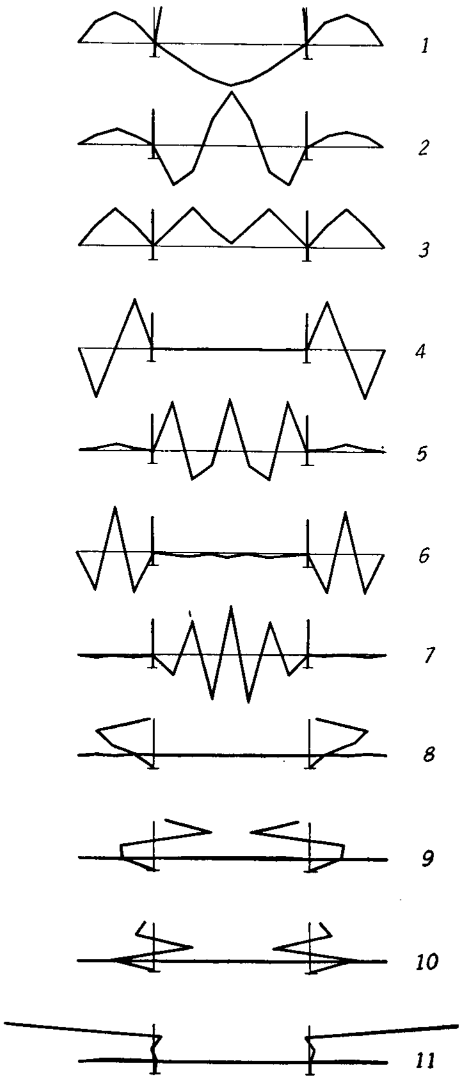

Fig. 6. Symmetric Modes.

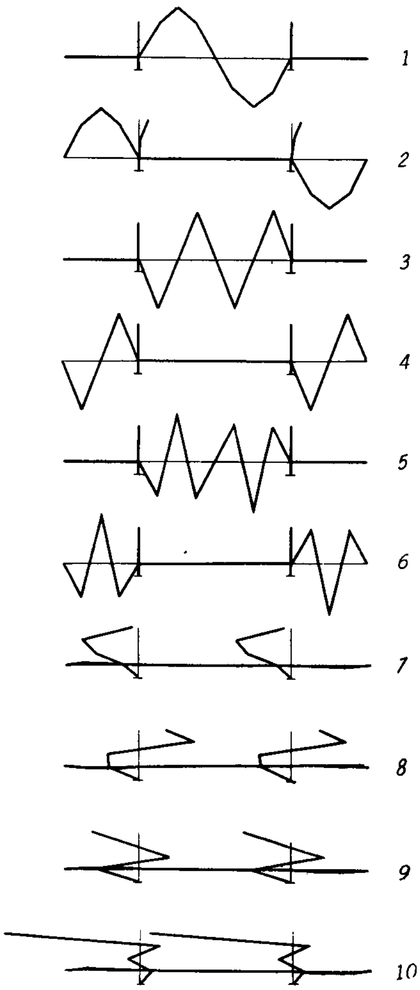

Fig. 7. Asymmetric Modes.

5. Application of Modal Analysis

Natural frequencies and modes of the system obtained in the preceding section will be utilized in the following analysis.

The displacement y_r of the system can be expressed as follows employing the normal modes obtained and new time functions $q_1, q_2, q_3, \cdots, q_n$.

$$y_r = q_1 Y_r^{(1)} + q_2 Y_r^{(2)} + q_3 Y_r^{(3)} + \cdots + q_n Y_r^{(n)} \qquad (24)$$

$$(r = 1, 2, 3, \cdots, n)$$

where, $Y_r^{(i)}$: amplitude of ith mode free vibration. Substituting Eq. (24) into Eq. (21), one obtains, after some calculations,

$$\ddot{q}_l+\lambda_l q_l+\sum_{i=1}^{n} Y_i^{(l)} P_i(t) = 0 \qquad (l = 1, 2, 3, \cdots, n) \tag{25}$$

provided that all the modes of vibration are normalized.

Each equation of the system of differential equations, Eq. (25), has a single dependent variable q_s and can be solved by ordinary method. If all q_s are given under the specific external force $P_r(t)$, the displacements can be obtained from Eq. (24).

6. Response to the Ground Motion

(a) Assumption of Ground Motion

Because of the great complexity of the earthquake motion, an exact solution of the earthquake responses of the suspension bridge is seldom possible, and only an approximate solution of the suspension bridge to some idealized ground motions are possible. In this paper, the ground motion is, as the first stage, assumed to be a displacement with a simple harmonic shape given as

$$\left.\begin{aligned} Z &= A\left(1-\cos\frac{2\pi}{T}t\right) && (0\leqslant t\leqslant T) \\ &= 0 && (t> T) \end{aligned}\right\} \tag{26}$$

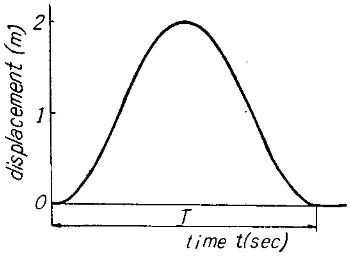

Fig. 8. External Disturbance.

and shown in Fig. 8. Responses to other kinds of disturbances can be obtained by this analysis, and it will be done in future work. In numerical analysis of this paper, the amplitude is assumed as $A=1$ m, then the maximum displacement of the ground motion is 2 m. Because of the linearity of the system considered response to any amplitude can be obtained by linear reduction.

(b) Response to the Ground Motion

In the design purpose, response of the bending moments in the system are much more significant than those of the displacement. The response of the bending moments on the following sections will be discussed in this paper: (1) the tower base, (2) the center of the tower, and (3) the center or the center span stiffening frame.

The ground motion of Eq. (26) can be applied to any points connecting the structure to the ground, those are left and right side cable anchorages and two tower bases, and each ground motion has an individual effect on the structure. Because the structure has long span lengths, any phase differences between each disturbance is possible. The responses in this chapter are obtained by adding the effect of each disturbance graphically so as to make the resultant bending moment maximum.

Fig. 9 (a) and (b) show the time-bending moment curves to the point of the center of the tower due to the disturbances with different durations of ground motions. $T=0.125$, 0.250, 0.375, (Fig. 9 (a)), 0.50, 0.75, 1.00, 1.50 (Fig. 9 (b)) in sec. Fig. 10 shows the time-bending moment curves for the center of the center span due to the same disturbances. In Fig. 10, are given fairly different response characteristics from Fig. 9, and the maximum moment is much less than that of the tower.

Fig. 11 shows the spectra for the maximum bending moment at the center of the tower resulting from the disturbance of eq. (23). Fig. 12 shows the spectra for the maximum bending moment at the tower base, and Fig. 13 shows the

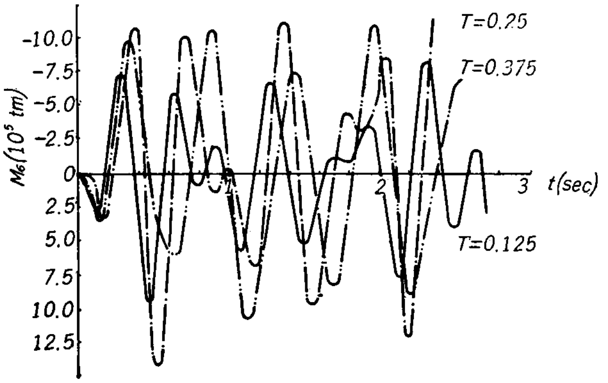

Fig. 9(a). Time-Bending Moment Curves.

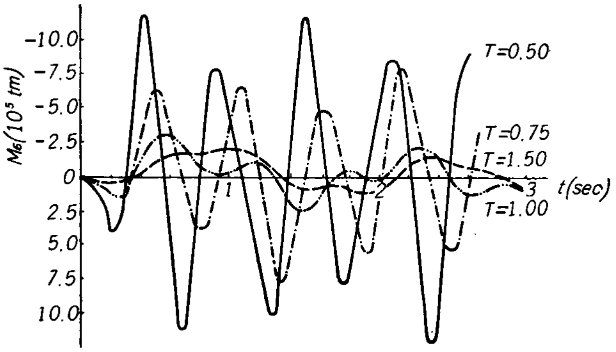

Fig. 9(b). Time-Bending Moment Curves.

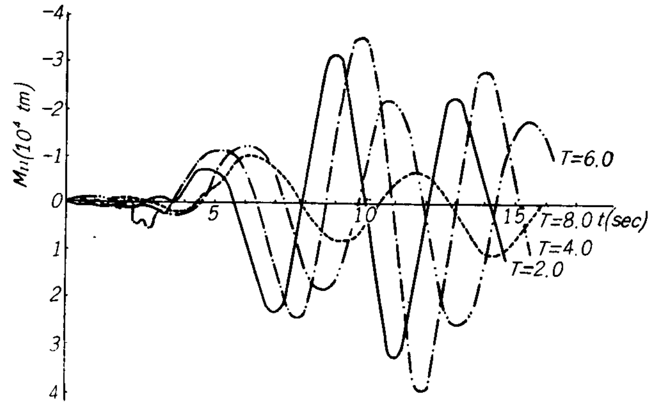

Fig. 10. Time-Bending Moment Curves.

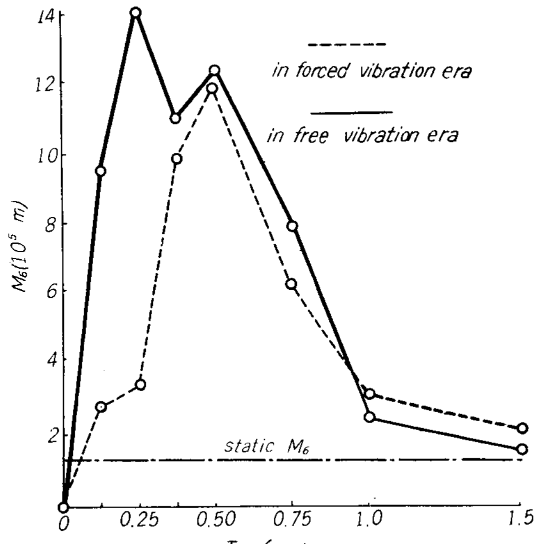

Fig. 11. Response Spectra (Tower).

spectra at the center of the center span stiffening frame. The spectra of Figs. 11 and 12 have their maximum values at about the value of $T=0.25$ sec. and Fig. 13, at about $T=4$ sec.

Patterns of the ground motions of earthquakes have to be given in order to get clear understanding on response spectra. If the amplitude and period in Eq. (26) are given, the response to the external disturbance, Eq. (26), can be obtained considering the linearity of the system.

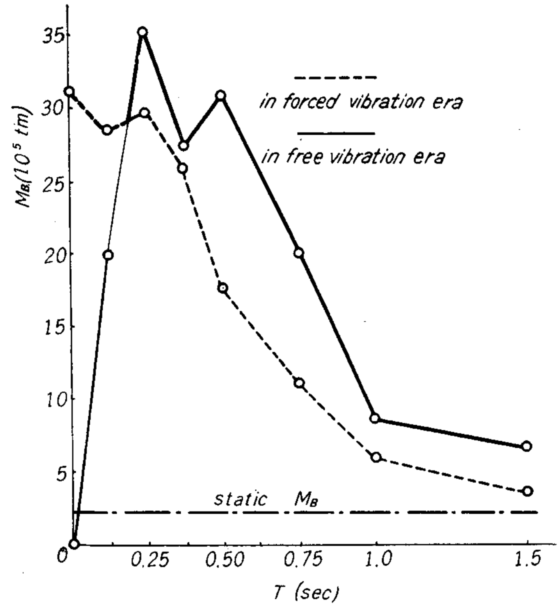

Fig. 12. Response Spectra (Tower).

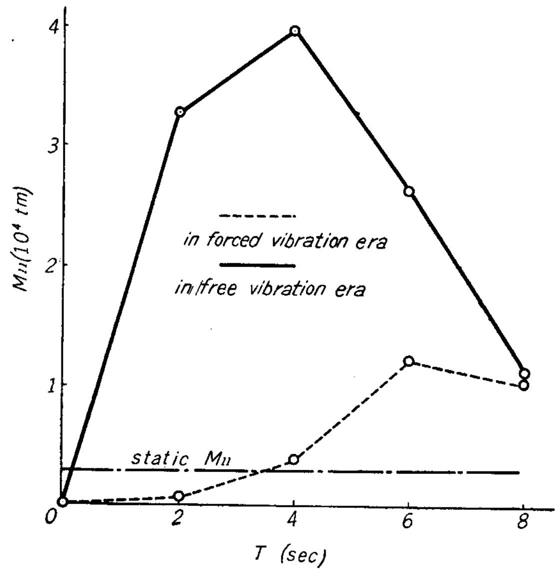

Fig. 13. Response Spectra (Stiffening Frame).

7. Conclusion

The response of the suspension bridge due to ground disturbances are analysed by adopting the simplified structural system with finite degrees of freedom, and some response spectra are obtained.

The main conclusions are:

(1) Vibration modes of the system, Figs. 6 and 7, can be separated into two groups with different characteristics. In one group, the displacement of the stiffening frames are predominent, such as the 1st through the 7th symmetric and the 1st through the 6th asymmetric modes, and in the other group, displacements of the towers are predominent, as the 8th through the 11th symmetric and the 7th through the 10th asymmetric modes.

(2) As it is clear from the response spectra, motions of the towers subjected to an earthquake are more significant than those of the stiffening frames, and the stiffness and masses of the towers must be taken into account in the analysis of earthquake response of suspension bridges.

(3) Two vibration modes of the tower, such as the 8th symmetric and the 7th asymmetric modes, are almost the same as shown in Figs. 6 and 7 excepting that they are symmetric and asymmetric. This means that in experimental and theoretical investigations of earthquake response, a partial model where only the tower and physically equivalent effects of cables and stiffening frames are considered is approximately applicable.

Only the fundamental characteristics were obtained, in this analysis, then the following experimental and theoretical investigations are necessary to obtain clear understanding on the problem and practical design.

(1) The same numerical analysis for the simplified system with better approximation than the system of Fig. 5 must be done to obtain design data for the suspension bridge. Natural modes and frequencies for the system having eight segments in the tower and the same number of segments as in Fig. 5 in the stiffening frames were obtained, and the dynamic response are now being calculated.

(2) The effects of the higher mode vibration to the bending moment of the tower were significant according to the numerical calculation done. Damping of the higher mode vibrations have to be clarified to obtain better information on higher mode responses because the damping effect is considered to be more effective to the higher mode vibrations than to the lower modes.

(3) Model tests on the tower has to be done to obtain the experimental results on earthquake response and damping characteristics.

(4) Analysis upon the deflection theory and the earthquake responses with plastic

deformations of the structure must be done, and the allowable plastic deformations of the suspension bridge must be made clear.

(5) Response due to earthquake with any directions of motion must be investigated.

Acknowledgement

The authors would like to express their sincere appreciations to Dr. Chujiro Haraguchi, Mayor of the City of Kobe, whom they owe so much for the completion of this work.

Bibliography

1) Newmark, N. M.; A Method of Computation for Structural Dynamics, Proc. of ASCE, **85**, EM, p. 67, (1959)
2) Bleich, Fr., McCullough, C. B., Rosecrans R., and Vincent, G. S.; The Mathematical Theory of Vibration in Suspension Bridges, U. S. Government Printing Office, p. 282 (1950)
3) Haraguchi, C.; The Proposed Suspension Bridge Over the Akashi Straits to Connect Kobe City with Awaji Island, Kobe City Authority (1959)
4) Timoshenko, S., Vibration Problems in Engineering, Second Edition, p. 209 (1939)